Drug Testing Applications

The development of artificial tissue/organs with the functional maturity of their native equivalents is one of the long-awaited panaceas for the medical and pharmaceutical industries. Advanced 3D cell printing technology and functional bioinks are promising innovations in the field of tissue engineering that have enabled the fabrication of complex, living 3D tissue/organs. Various requirements for these tissues, including complex and large-volume structure, tissue-specific microenvironments, and functional vasculatures, have been addressed to engineer tissue/organs with the functionality of native tissue. Tissue/organ constructs that satisfy such criteria may facilitate the development of reliable in vitro testing platforms for drug development.

1. Introduction

Since the first cell culture was reported by Ross Harrison, cellular engineering has advanced through the development of various animal/plant cell culture methods, the establishment of useful cell lines, the discovery of stem cells, and reprogramming technologies for the production of induced pluripotent stem cells (iPSCs) and other cells of interest [1][2]. When 3D cultivation methods were reported in the early twenty-first century, various biomaterials and scaffolds were introduced to the conventional cell culture techniques to provide 3D environments beyond the culture plate and modulate behaviors of the cells [3][4][5]. The cell-based constructs using these complex approaches have shown improved performance compared to conventional 2D culture methods by providing an environment that mimics native tissue. Many studies have also been conducted on the feasibility of using this technique to develop functional tissue/organs in the field of tissue regeneration and in vitro models [6][7][8].

An early type of cell-based construct was fabricated by seeding cells on a porous scaffold to be used for clinical and pharmaceutical applications [9][10][11]. Various techniques and materials were used to fabricate the tissue/organ mimetic structure, the scaffold, and then cells were seeded manually [12][13][14]. Using this method, several types of tissue, including cartilage, bone, and skin were developed and showed significant advances in the treatment of partial defects [15][16][17]. However, due to limitations in the areas of multi-cellular interaction, vascularization, and the creation of a complex physiological environment, there are challenges in regenerating large defects and developing therapeutics for native tissue/organs with complex cell arrangements and architectures such as the liver, lung, and kidney.

To overcome these limitations, 3D cell printing has been researched due to its ability to precisely deposit various biomaterials and living cells according to their native equivalents [18][19][20]. The 3D structure is fabricated by stacking 2D patterns in layers during the printing process. This automated system provides a precisely controlled structure with high reproducibility [21][22][23]. Moreover, advanced control systems have enabled 3D printing techniques to dispense live cells [24][25]. Advances in medical imaging technology, including computed tomography and magnetic resonance imaging, have also improved 3D cell printing [26][27][28]. These new technologies facilitate the fabrication of complex structures via computer-aided design (CAD) and computer-aided manufacturing (CAM) processes based on medical imaging.

In addition to novel fabrication methods, the development and advancement of bioink, which is a printable biomaterial capable of encapsulating cells, has also contributed to preserving 3D structure, providing a suitable biochemical environment for printed cells, and protecting cells from harsh conditions during the printing process [29][30]. Therefore, the combination of 3D cell printing technology and functional bioinks could meet the physical, chemical, and biological requirements for developing living tissue/organs [31]. To date, various types of 3D-printed functional tissue/organs have shown the potential for successful transplantation [32]. Also, the printed construct has been studied for in vitro tissue/organ models for testing platforms in the pharmaceutical industry to detect drug-induced toxicity or to validate the drug efficacy for the target diseases [33]. These applications of 3D printing techniques are expected to advance drug development and reduce the number of patients suffering from a global organ shortage.

2. Drug Screening Applications

Animal models are widely used to test drugs. However, differences in physiology, pharmacokinetics, and genetics reduce the reliability of animal models [34]. Although humans and mice share the same genes, their regulation mechanism is different [35]. Drug testing results vary according to which species is used [36][37]. Therefore, there is a significant demand for models made of human cells as an alternative to animal models. Furthermore, if patient-derived cells are used to produce drug-testing models, it is possible to produce personalized medicine. To fabricate a physiologically relevant model, researchers have focused on recreating complex architecture and cell-cell interactions [38][39]. Thus, 3D cell printing is a promising technology for achieving these objectives.

Because the liver and kidney are susceptible to drug-induced injury, drug toxicity is a crucial consideration when developing new drugs. To produce drug toxicity testing platforms, there have been several attempts to replicate the complex tubular structures of the liver and kidney using 3D cell printing technology. In addition, due to the restrictions on animal testing in the cosmetic industry, in vitro skin models have been developed relatively earlier than other tissues. The utility of 3D cell printing for the fabrication of full-thickness skin models has been demonstrated by several studies. 3D cell printing also has the advantages of cost-effectiveness and the ability to customize production. These characteristics have synergistic effects with the use of patient-derived cells to personalize medicine. For example, 3D-printed cancer models have been developed to create personalized disease models for patient-specific drug efficacy tests.

2.1. Liver Model

The liver is a major organ that regulates the overall metabolism in the body and plays a crucial role in pharmacokinetics/pharmacodynamics (PK/PD) of drugs by taking charge of biotransformation [40]. This makes hepatotoxicity a critical safety issue to consider in drug development. Therefore, it is essential to develop an in vitro hepatic model with the functional maturity to precisely simulate and anticipate the behavior of various substances in the liver. Many researchers have applied 3D printing technology to produce mature hepatic functions by mimicking a hexagonal lobule and hepatic sinusoidal structure where the hepatocyte and blood vessel are aligned in a specific manner. For example, Bhise et al. used 3D printing technology to create an in vitro hepatic model using a photocurable GelMA bioink [41]. In the study, hepatic spheroids encapsulated in GelMA were printed and cultured on a PDMS-based bioreactor with a hexagonal shape and continuous perfusion. Hepatic markers such as albumin, A1AT, and transferrin were maintained for 4 weeks, and significant hepatic toxicity was observed in acetaminophen treatment for 6 days, indicating its feasibility as a drug testing platform.

Taking into account the multi-cellular components and microstructure of the liver, Lee et al. developed a one-step 3D-printed liver-on-a-chip consisting of compartmentalized parts of a hepatocyte and vessel and a PCL chip body [42]. The vascular part of the monolayer was achieved by printing the endothelial cells encapsulated in gelatin bioink, and the hepatic sinusoid-mimicking channel was produced. In the hepatic model with a monolayer vascular portion and culture media perfusion through the microchannel, the viability and synthesis of albumin and urea were significantly improved (Figure 1A).
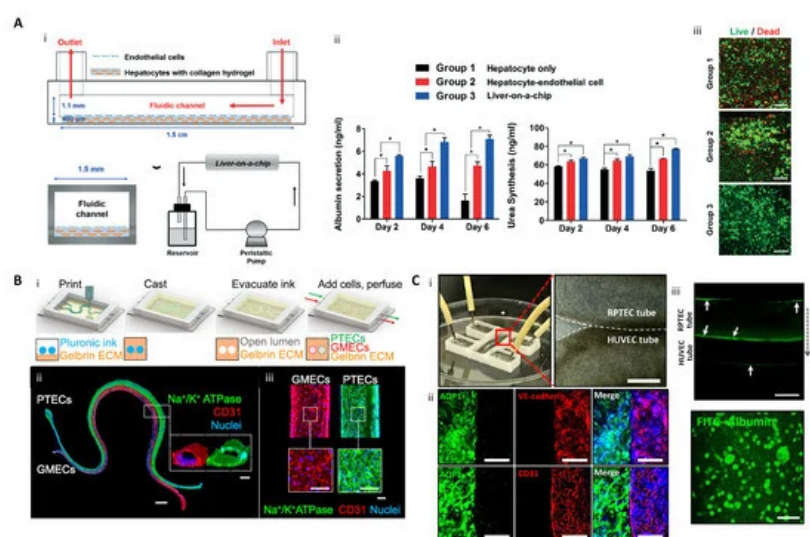

Figure 1. 3D printed liver-on-a-chip and kidney-on-a-chip. (**A**) 3D printing-based liver-on-a-chip (i) Schematic diagram of one-step fabricated liver-on-a-chip with a vascular channel; (ii) Liver function analysis with albumin and urea tests (* $p < 0.05$); (iii) hepatocyte viability on Day 6 (scale bar: 100 μm) (reproduced with permission from ref [42]; published by The Royal Society of Chemistry). (**B**) 3D vascularized proximal tubule on a chip (3D VaPT) model; (i) Fabrication process of

the 3D VaPT model; (ii) The fluorescence image of the 3D VaPT model. PTECs are presented in blue, GMECs in red, and nuclei in blue (Scale bar: 1 mm). The cross-sectional views of each microchannel (scale bar: 100 μm); (iii) Magnification of PTECs and GMECs channel in the 3D VaPT model (scale bar: 100 μm). (**C**) 3D cell-printed renal proximal tubule-on-a-chip with tubular RTPEC and HUVEC constructs. (i) Microfluidic system and dual tubular constructs of the chip after fabrication; (ii) Fluorescence image of renal proximal tubular markers (AQP1, aquaporin 1), and vascular markers (vascular endothelial (VE)-cadherin, and CD31) in the chip after maturation. The renal proximal tubular marker is presented in green, vascular endothelial markers are red, and nuclei are blue (scale bar: 100 μm); (iii) Albumin reabsorption between RTPEC and HUVEC tube via vectorial transport. Arrows indicate the intracellular accumulating albumin within the RPTEC and sidewall of the vessel (scale bar: 400 μm) (reproduced with permission from ref [43]; copyright 2020 Elsevier).

While the previous study was a pump-based chip, the same research group reported a liver-on-a-chip with a biochemical microenvironment and biliary system [44]. In the chip, liver dECM bioink and a hepatic progenitor cancer cell line were used for the biochemical environment and biliary structure, respectively, and pumpless fluidics were used for more convenient operation. In the experimental group with a system for washing bile acid that causes hepatic toxicity, the expression of liver functional markers such as albumin, AFT, and TTR was upregulated, and the expression of CYPs related to drug metabolism increased. Moreover, the drug sensitivity using acetaminophen increased, as in the native liver, compared to the conventional 2D model.

2.2. Kidney Model

Although some drugs used for medical treatment can cause nephrotoxicity, there are many cases where they are inevitably used [45]. In addition, renal toxicity of drug candidates is found relatively later in the drug development process, leading to an increase in the cost of developing new drugs [46]. Therefore, a human renal tissue model is urgently required. Researchers developing renal tissue in vitro have produced complicated and perfusable renal tubular constructs using 3D printing technology. The kidney is made up of a functional unit called a nephron, where tubular structures such as proximal tubules, glomeruli, and blood vessels are compartmentalized and interact closely, and 3D printing technology has enabled the replication of such complicated renal structures.

LIN, Neil YC, et al. developed a 3D vascularized proximal tubule model with a perfusable proximal tubule and blood vessel constructs [47]. First, a dual-microchannel portion was printed with a fugitive bioink composed of Pluronic F127 and high-molecular-weight poly(ethylene oxide). Then, a hydrogel composed of gelatin and fibrinogen was poured and crosslinked. After that, the renal proximal tubular epithelial cells (RPTECs) and glomerular microvascular endothelial cells were seeded in each microchannel produced by removing the fugitive bioinks. These matured into a vascularized renal tubular model capable of perfusion. This construct enabled substance exchange, such as albumin reabsorption and glucose reabsorption, between the proximal tubule and blood vessels, which was not possible with conventional models (Figure 1B).

Singh et al. developed a vascularized kidney-on-a-chip consisting of a renal proximal tubule and blood vessels. This was achieved using direct, coaxial cell-printing and a hybrid bioink made of kidney dECM and alginate [43]. The hybrid bioink improved the viability and the expression of functional markers such as gamma-glutamyl transpeptidase (GGT), aquaporin 1 (AQP1), and kidney-specific cadherin (KSP) in RPTECs compared to using medical-grade collagen type I bioink. In addition, the expression of functional markers in the proximal tubule was upregulated compared to the conventional 2D and 3D culture methods, indicating that the tubular architecture was also a specialized cue for functional maturation of the renal proximal tubule. A vascularized renal proximal tubule-on-a-chip was fabricated by printing the proximal and vascular tubes close together but compartmentalized on the chip body made of PCL. When the culture media was perfused in each tube, receptor-mediated endocytosis of FITC-albumin was observed, confirming that native-like renal behavior was achieved (Figure 1C).

2.3. Skin Model

The European Union's ban on animal testing for cosmetic products has accelerated the development of in vitro skin models to replace animal testing. The skin consists of dermis, epidermis, and hypodermis, and plays an important role in temperature regulation, tactile sensing, and acting as a physical barrier. It also contains a vascular network, nerves, and appendages such as hair, glands, and nails. To develop cosmetics and drugs to be applied to skin, in vitro skin models must mimic the complexity of native skin, and 3D cell printing technology can be utilized to replicate this complex 3D anatomy.

Pourchet, Léa J., et al. produced dermis analogs by printing human dermal fibroblasts using a mixture of gelatin, alginate, and fibrinogen as a bioink, and seeding human epidermal keratinocytes on a dermis structure to create a skin model. After 26 days of culture, the morphology of the mature skin model was similar to that of human skin (Figure 2A) [48]. ECM plays an important role in enhancing cell-cell interaction, and cell-ECM interactions are important for developing epidermal organization. Accordingly, to promote cell activity and their interaction, Kim et al. used skin dECM bioink that produces a native-like microenvironment to print an in vitro dermal/epidermal skin model. Fibroblasts in skin dECM bioink showed better cell behavior for skin regeneration than collagen type 1 bioink. The skin dECM bioink produced less contraction of the dermis structure that occurs during the maturation process. In contrast to collagen type 1 bioink, this characteristic improved the epidermal organization. The prevention of tissue contraction was due to the presence of thick collagen fibers and ECM components, such as elastin and hyaluronic acid, in the skin dECM bioink. This skin dECM bioink enabled the fabrication of an in vitro model that is closer to the native skin in terms of its barrier function compared to collagen type 1 bioink (Figure 2B) [49].
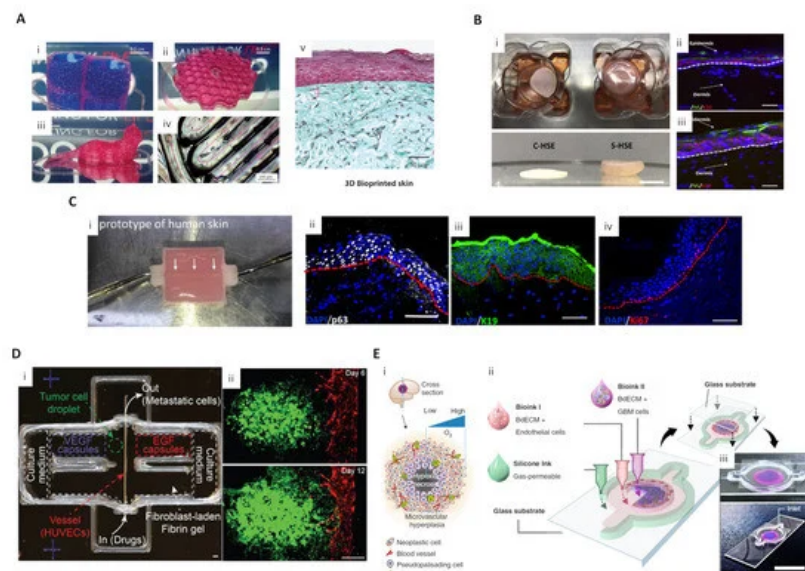

Figure 2. 3D-printed skin and cancer model for drug screening applications (**A**) Diverse-shaped 3D-printed structures using a scaffold-free approach with gelatin-alginate-fibrinogen bioink and 3D-printed skin. (i) A water-tight structure with two compartments filled with blue dyed liquid; (ii) A complex structure with hollow honeycomb features of 200 μm width; (iii) A centimeter-sized complex object with overhanging structures; (iv) A closer view of a print showing 200 μm wide printing lines. Pink arrows show the printing movement of the nozzle; (v) Optical microscopy of Masson's Trichrome images of bioprinted skin after 26 d of culture (reproduced with permission from ref [48]; copyright 2017 Wiley-VCH). (**B**) 3D-printed skin using skin dECM bioink. (i) Representative photographs of 3D cell-printed in vitro skin equivalents using type I collagen (C-HSE) and skin-derived bioink (S-HSE); (ii, iii) Expression of epidermal differentiation markers with C-HSE (ii) and S-HSE (iii) on Day 10 after ALI culture (reproduced with permission from ref [49]; copyright 2018 Elsevier). (**C**) Perfusable vascularized skin equivalent composed of epidermis, dermis, and hypodermis. (i) A prototype of the fabricated perfusable full-thickness skin construct, (ii) immunostaining of p63 (white), (iii) K19 (green), and (iv) Ki67 (red) in the skin construct (reproduced with permission from Ref [50]; copyright 2019 Wiley-VCH). (**D**) 3D-printed in vitro metastatic model. (i) Photo of a 3D-printed culture chamber to test guided tumor cell dissemination; (ii) Fluorescence images of a metastatic model on Days 6 and 12, showing that A549s approach and enter the vasculature through the fibroblast-laden fibrin gel (green channel: GFP-expressing A549s, red channel: RFP-expressing HUVECs) (reproduced with permission from ref [51]; copyright 2019 Wiley-VCH). (**E**) (i) Schematic illustration of a cross-sectional view of a native GBM; (ii) Schematic illustration of the process for printing the GBM-on-a-chip with various bioinks and other materials to construct a compartmentalized structure; (iii) Photographs of a mock GBM-on-a-chip (reproduced with permission from Ref [52]; copyright 2019 Nature Publishing Group).

The same research group developed a 3D-printed skin model, based on skin dECM bioink, with perfused blood vessels in the dermis and hypodermis sections. A PCL-based transwell platform was suggested to integrate the perfusable channel between the dermal and hypodermal compartments, and the gelatin-based vascular bioink was used to print a vessel-like channel with an endothelial cell monolayer. The maturation of this skin model was structurally assessed using functional markers representing the epidermis (stratified structure), dermis (dermal-epidermal junction, secreted ECM composition), hypodermis (lipid droplets), and vascular channels (endothelium). These experiments demonstrated a successful maturation of skin tissue. Moreover, histological analysis of a skin stemness marker showed that the skin model containing vascularized hypodermis and dermis shared more structural similarities with native human skin than the control group (Figure 2C) [50].

In addition to keratinocytes, skin epidermis also contains melanocytes, which are critical for skin pigmentation. Traditional methods of pigmented 3D skin fabrication are limited in their ability to produce uniform skin pigmentation. Ng et al. demonstrated the advantage of 3D cell printing to overcome this limitation. Using an inkjet printing system, the dermal portion was printed with fibroblast-laden collagen bioink, and keratinocytes and melanocytes were printed on the dermal construct. Compared to the conventional manual-casting approach, the 3D-printed pigmented skin construct had greater similarity to native skin tissue in the presence of well-developed stratified epidermal layers and the presence of a permanent basement membrane layer [53].

2.4. Cancer Model

Cancer is among the leading causes of death worldwide, and differences between in vitro and in vivo efficacy is still a major limitation in the development of effective drugs and therapies [54]. Therefore, advanced cancer treatment will require a clinically applicable model. Furthermore, many studies have been conducted on the toxicity of anticancer drugs, making this a high-priority area of development for pharmaceuticals. Cancer growth and progression are affected substantially by complex microenvironments, including multiple cell types, different types of ECM molecules, and their interactions. 3D bioprinting techniques have been utilized to create tumor micro-environments because of their advantages in this application such as precise composition and well-organized spatial distribution of tumor cells and extracellular components.

Meng et al. developed 3D metastatic in vitro printed models with a precisely controlled spatial positioning of cells, programmable growth factor release capsules, and biomaterials. The growth factor gradient was controlled using programmable release capsules triggered by laser irradiation to mimic tumor metastasis and angiogenesis. After guided migration of tumor cells and endothelial cells, the efficacy of immunotoxin was tested to demonstrate the utility of the 3D vascularized cancer model as a drug screening platform (Figure 2D) [51].

Furthermore, 3D cell printing technology also showed the potential to simulate multi-tissue/organ metastasis since it enables the deposition of different tissues in one platform. Cui et al. simulated breast cancer metastasis to bone tissue using an SLA 3D printing system with bioink optimized for cancer cells, endothelial cells, and osteoblasts. This system enabled the observation of transendothelial migration and colonization of cancer cells in vitro [55]. Yi et al. 3D printed glioblastoma-on-a chip to study patient-specific responses to chemoradiotherapy. Brain dECM bioink was used to encapsulate patient-derived tumor cells and endothelial cells and print a compartmentalized cancer-stroma concentric-ring structure. The printed cancer model sustains a physiologically relevant radial oxygen gradient by combining a 3D-printed gas-permeable silicon wall and a glass coverslip. This model effectively mimicked the architectural, biophysical, and biochemical characteristics of natural glioblastoma tumors. The study also observed patient-specific resistance to temozolomide and chemoradiation therapy and patient-specific sensitivity to potential combinations of anti-cancer drugs (Figure 2E) [52].

References

1. Jedrzejczak-Silicka, M. History of cell culture. In New Insights into Cell Culture Technology; Intech: Rijeka, Croatia, 2017.

2. Rodríguez-Hernández, C.O.; Torres-Garcia, S.E.; Olvera-Sandoval, C.; Ramirez-Castillo, F.Y.; Muro, A.L.; Avelar-Gonzalez, F.J.; Guerrero-Barrera, A.L. Cell culture: History, development and prospects. Int. J. Curr. Res. Acad. Rev. 2014, 2, 188–200.

3. Huh, D.; Hamilton, G.A.; Ingber, D.E. From 3D cell culture to organs-on-chips. Trends Cell Biol. 2011, 21, 745–754.

4. Pampaloni, F.; Reynaud, E.G.; Stelzer, E.H.K. The third dimension bridges the gap between cell culture and live tissue. Nat. Rev. Mol. Cell Biol. 2007, 8, 839–845.

5. Haycock, J.W. 3D Cell Culture: A Review of Current Approaches and Techniques; Springer Science and Business Media LLC: Amsterdam, The Netherlands, 2010; Volume 695, pp. 1–15.

6. Khademhosseini, A.; Langer, R. A decade of progress in tissue engineering. Nat. Protoc. 2016, 11, 1775–1781.

7. Edmondson, R.; Broglie, J.J.; Adcock, A.F.; Yang, L. Three-Dimensional Cell Culture Systems and Their Applications in Drug Discovery and Cell-Based Biosensors. ASSAY Drug Dev. Technol. 2014, 12, 207–218.

8. Maltman, D.J.; Przyborski, S.A. Developments in three-dimensional cell culture technology aimed at improving the accuracy of in vitro analyses. Biochem. Soc. Trans. 2010, 38, 1072–1075.

9. Holy, C.E.; Shoichet, M.S.; Davies, J.E. Engineering three-dimensional bone tissuein vitro using biodegradable scaffolds: Investigating initial cell-seeding density and culture period. J. Biomed. Mater. Res. 2000, 51, 376–382.

10. Vunjak-Novakovic, G.; Obradovic, B.; Martin, I.; Bursac, P.M.; Langer, R.; Freed, L.E. Dynamic Cell Seeding of Polymer Scaffolds for Cartilage Tissue Engineering. Biotechnol. Prog. 1998, 14, 193–202.

11. Dar, A.; Shachar, M.; Leor, J.; Cohen, S. Optimization of cardiac cell seeding and distribution in 3D porous alginate scaffolds. Biotechnol. Bioeng. 2002, 80, 305–312.

12. O'Brien, F.J. Biomaterials & scaffolds for tissue engineering. Mater. Today 2011, 14, 88–95.

13. Chan, B.P.; Leong, K.W. Scaffolding in tissue engineering: General approaches and tissue-specific considerations. Eur. Spine J. 2008, 17, 467–479.

14. Dhandayuthapani, B.; Yoshida, Y.; Maekawa, T.; Kumar, D.S. Polymeric Scaffolds in Tissue Engineering Application: A Review. Int. J. Polym. Sci. 2011, 2011, 1–19.

15. Vinatier, C.; Bouffi, C.; Merceron, C.; Gordeladze, J.; Brondello, J.-M.; Jorgensen, C.; Weiss, P.; Guicheux, J.; Noel, D. Cartilage Tissue Engineering: Towards a Biomaterial-Assisted Mesenchymal Stem Cell Therapy. Curr. Stem Cell Res. Ther. 2009, 4, 318–329.

16. Zhang, Y.; Venugopal, J.R.; El-Turki, A.; Ramakrishna, S.; Su, B.; Lim, C.T. Electrospun biomimetic nanocomposite nanofibers of hydroxyapatite/chitosan for bone tissue engineering. Biomaterials 2008, 29, 4314–4322.

17. MacNeil, S. Progress and opportunities for tissue-engineered skin. Nat. Cell Biol. 2007, 445, 874–880.

18. Mironov, V.; Reis, N.; Derby, B. Review: Bioprinting: A Beginning. Tissue Eng. 2006, 12, 631–634.

19. Park, J.Y.; Gao, G.; Jang, J.; Cho, D.-W. 3D printed structures for delivery of biomolecules and cells: Tissue repair and regeneration. J. Mater. Chem. B 2016, 4, 7521–7539.

20. Park, J.H.; Jang, J.; Lee, J.-S.; Cho, D.-W. Three-Dimensional Printing of Tissue/Organ Analogues Containing Living Cells. Ann. Biomed. Eng. 2016, 45, 180–194.

21. Kang, H.-W.; Park, J.H.; Kang, T.-Y.; Seol, Y.-J.; Cho, D.-W. Unit cell-based computer-aided manufacturing system for tissue engineering. Biofabrication 2012, 4, 015005.

22. Jung, J.W.; Park, J.H.; Hong, J.M.; Kang, H.-W.; Cho, D.-W. Octahedron pore architecture to enhance flexibility of nasal implant-shaped scaffold for rhinoplasty. Int. J. Precis. Eng. Manuf. 2014, 15, 2611–2616.

23. George, E.; Liacouras, P.; Rybicki, F.J.; Mitsouras, D. Measuring and Establishing the Accuracy and Reproducibility of 3D Printed Medical Models. Radiographics 2017, 37, 1424–1450.

24. Murphy, S.V.; Atala, A. 3D bioprinting of tissues and organs. Nat. Biotechnol. 2014, 32, 773–785.

25. Karzyński, K.; Kosowska, K.; Ambrozkiewicz, F.; Berman, A.; Cichoń, J.; Klak, M.; Serwanska-Swietek, M.; Wszoła, M. Use of 3D bioprinting in biomedical engineering for clinical application. Med. Stud. 2018, 34, 93–97.

26. Kang, H.-W.; Lee, S.J.; Ko, I.K.; Kengla, C.; Yoo, J.J.; Atala, A. A 3D bioprinting system to produce human-scale tissue constructs with structural integrity. Nat. Biotechnol. 2016, 34, 312–319.

27. Yi, H.-G.; Choi, Y.-J.; Jung, J.W.; Jang, J.; Song, T.-H.; Chae, S.; Ahn, M.; Choi, T.H.; Rhie, J.-W.; Cho, D.-W. Three-dimensional printing of a patient-specific engineered nasal cartilage for augmentative rhinoplasty. J. Tissue Eng. 2019, 10.

28. Jung, J.W.; Ha, D.-H.; Kim, B.-Y.; Seo, B.F.; Han, H.H.; Kim, D.H.; Rhie, J.-W.; Kim, S.W.; Cho, D.-W. Nasal Reconstruction Using a Customized Three-Dimensional-Printed Stent for Congenital Arhinia: Three-Year Follow-up. Laryngoscope 2018, 129, 582–585.

29. Groll, J.; Burdick, J.A.; Kim, Y.K.; Derby, B.; Gelinsky, M.; Heilshorn, S.C.; Jüngst, T.; Malda, J.; A Mironov, V.; Nakayama, K.; et al. A definition of bioinks and their distinction from biomaterial inks. Biofabrication 2018, 11, 013001.

30. Axpe, E.; Oyen, M.L. Applications of Alginate-Based Bioinks in 3D Bioprinting. Int. J. Mol. Sci. 2016, 17, 1976.

31. Jang, J.; Park, J.Y.; Gao, G.; Cho, D.-W. Biomaterials-based 3D cell printing for next-generation therapeutics and diagnostics. Biomaterials 2018, 156, 88–106.

32. Arslan-Yildiz, A.; El Assal, R.; Chen, P.; Guven, S.; Inci, F.; Demirci, U. Towards artificial tissue models: Past, present, and future of 3D bioprinting. Biofabrication 2016, 8, 014103.

33. Jang, J.; Yi, H.-G.; Cho, D.-W. 3D Printed Tissue Models: Present and Future. ACS Biomater. Sci. Eng. 2016, 2, 1722–1731.

34. Akhtar, A. The Flaws and Human Harms of Animal Experimentation. Camb. Q. Healthc. Ethics 2015, 24, 407–419.

35. Hodge, R.D.; Bakken, T.E.; Miller, J.A.; Harcourt-Smith, W.E.H.; Barkan, E.R.; Graybuck, L.T.; Close, J.L.; Long, B.; Johansen, N.; Penn, O.; et al. Conserved cell types with divergent features in human versus mouse cortex. Nat. Cell Biol. 2019, 573, 61–68.

36. Van Norman, G.A. Limitations of Animal Studies for Predicting Toxicity in Clinical Trials: Is it Time to Rethink Our Current Approach? JACC Basic Transl. Sci. 2019, 4, 845–854.

37. Van Norman, G.A. Limitations of Animal Studies for Predicting Toxicity in Clinical Trials: Part 2: Potential Alternatives to the Use of Animals in Preclinical Trials. JACC Basic Transl. Sci. 2020, 5, 387–397.

38. Lin, A.; Skottvoll, F.S.; Rayner, S.; Pedersen-Bjergaard, S.; Sullivan, G.; Krauss, S.; Wilson, S.R.; Harrison, S. Back cover: 3D cell culture models and organ-on-a-chip: Meet separation science and mass spectrometry. Electrophoresis 2020, 41, 56–64.

39. Achberger, K.; Probst, C.; Haderspeck, J.; Bolz, S.; Rogal, J.; Chuchuy, J.; Nikolova, M.; Cora, V.; Antkowiak, L.; Haq, W.; et al. Merging organoid and organ-on-a-chip technology to generate complex multi-layer tissue models in a human retina-on-a-chip platform. eLife 2019, 8, 46188.

40. Eddershaw, P.J.; Beresford, A.P.; Bayliss, M.K. ADME/PK as part of a rational approach to drug discovery. Drug Discov. Today 2000, 5, 409–414.

41. Bhise, N.S.; Manoharan, V.; Massa, S.; Tamayol, A.; Ghaderi, M.; Miscuglio, M.; Lang, Q.; Zhang, Y.S.; Shin, S.R.; Calzone, G.; et al. A liver-on-a-chip platform with bioprinted hepatic spheroids. Biofabrication 2016, 8, 014101.

42. Lee, H.; Cho, D.-W. One-step fabrication of an organ-on-a-chip with spatial heterogeneity using a 3D bioprinting technology. Lab Chip 2016, 16, 2618–2625.

43. Singh, N.K.; Han, W.; Nam, S.A.; Kim, J.W.; Kim, J.Y.; Kim, Y.K.; Cho, D.-W. Three-dimensional cell-printing of advanced renal tubular tissue analogue. Biomaterials 2020, 232, 119734.

44. Lee, H.; Chae, S.; Kim, J.Y.; Han, W.; Kim, J.; Choi, Y.-J.; Cho, D.-W. Cell-printed 3D liver-on-a-chip possessing a liver microenvironment and biliary system. Biofabrication 2019, 11, 025001.

45. Bicalho, M.D.; Soares, D.B.; Botoni, F.A.; Reis, A.M.M.; Martins, M.A.P. Drug-Induced Nephrotoxicity and Dose Adjustment Recommendations: Agreement Among Four Drug Information Sources. Int. J. Environ. Res. Public Healthc. 2015, 12, 11227–11240.

46. Kandasamy, K.; Chuah, J.K.C.; Su, R.; Huang, P.; Eng, K.G.; Xiong, S.; Li, Y.; Chia, C.S.; Loo, L.-H.; Zink, D. Prediction of drug-induced nephrotoxicity and injury mechanisms with human induced pluripotent stem cell-derived cells and machine learning methods. Sci. Rep. 2015, 5, 12337.

47. Lin, N.Y.C.; Homan, K.A.; Robinson, S.S.; Kolesky, D.B.; Duarte, N.; Moisan, A.; Lewis, J.A. Renal reabsorption in 3D vascularized proximal tubule models. Proc. Natl. Acad. Sci. USA 2019, 116, 5399–5404.

48. Pourchet, L.J.; Thépot, A.; Albouy, M.; Courtial, E.J.; Boher, A.; Blum, L.J.; Marquette, C.A. Human Skin 3D Bioprinting Using Scaffold-Free Approach. Adv. Healthc. Mater. 2016, 6, 1601101.

49. Kim, B.S.; Kwon, Y.W.; Kong, J.-S.; Park, G.T.; Gao, G.; Han, W.; Kim, M.-B.; Lee, H.; Kim, J.H.; Cho, D.-W. 3D cell printing of in vitro stabilized skin model and in vivo pre-vascularized skin patch using tissue-specific extracellular matrix bioink: A step towards advanced skin tissue engineering. Biomaterials 2018, 168, 38–53.

50. Kim, B.S.; Gao, G.; Kim, J.Y.; Cho, D.-W. 3D Cell Printing of Perfusable Vascularized Human Skin Equivalent Composed of Epidermis, Dermis, and Hypodermis for Better Structural Recapitulation of Native Skin. Adv. Healthc. Mater. 2018, 8, e1801019.

51. Meng, F.; Meyer, C.M.; Joung, D.; Vallera, D.A.; McAlpine, M.C.; Panoskaltsis-Mortari, A. 3D Bioprinted In Vitro Metastatic Models via Reconstruction of Tumor Microenvironments. Adv. Mater. 2019, 31, e1806899.

52. Yi, H.-G.; Jeong, Y.H.; Kim, Y.; Choi, Y.-J.; Moon, H.E.; Park, S.-H.; Kang, K.S.; Bae, M.; Jang, J.; Youn, H.; et al. A bioprinted human-glioblastoma-on-a-chip for the identification of patient-specific responses to chemoradiotherapy. Nat. Biomed. Eng. 2019, 3, 509–519.

53. Naing, M.W.; Qi, J.T.Z.; Yeong, W.Y.; Naing, M.W. Proof-of-concept: 3D bioprinting of pigmented human skin constructs. Biofabrication 2018, 10, 025005.

54. Vanderburgh, J.; Sterling, J.A.; Guelcher, S.A. 3D Printing of Tissue Engineered Constructs for In Vitro Modeling of Disease Progression and Drug Screening. Ann. Biomed. Eng. 2016, 45, 164–179.

55. Cui, H.; Esworthy, T.; Zhou, X.; Hann, S.Y.; Glazer, R.I.; Li, R.; Zhang, L.G. Engineering a Novel 3D Printed Vascularized Tissue Model for Investigating Breast Cancer Metastasis to Bone. Adv. Healthc. Mater. 2019, 9, 1900924.